Evaluation of integrated tuning elements with SIS devices.

M.M.T.M. Dierichs[1], C.E. Honingh[2], R.A. Panhuyzen[2], B.J. Feenstra[1], A. Skalare[2,3], J.J. Wijnbergen[2], H. v.d. Stadt[2], Th. de Graauw[2].

1: Dept. of Applied Physics and Materials Science Centre, University of Groningen, Nijenborgh 4, 9747 AG Groningen, The Netherlands.

2: Space Research Organization of the Netherlands, Groningen, Landleven 12, 9747 AD Groningen, The Netherlands.

3: Dept. of Applied Electron Physics, Chalmers University of Technology, Göteborg, Sweden.

Abstract.

The resonance of integrated tuning stubs in combination with SIS detectors is measured and modeled. The predicted resonances are compared with measurements of stubs integrated with $Nb/Al_2O_3/Nb$ junctions in a log-periodic antenna using a Michelson interferometer. Different stub lengths were made on different substrates (on 200 μm thick quartz and on a 7 μm thick silicon membrane) and the results show a fairly good

agreement with the model calculations. Quartz substrates showed resonances up to 580 GHz, silicon membrane stub resonances reach as high as 480 GHz. An observed resonance at 560 GHz is probably a substrate effect from the membrane. The gap frequency for all the samples is 650 GHz and no resonances are detected above this frequency. Up to the maximum detected frequency dispersion is found to be negligible.

I Introduction.

SIS mixers with $Nb/Al_2O_3/Nb$ junctions are very sensitive submm detectors. Recent progress in SIS mixer development is due to the ability to manufacture smaller junctions down to sub-micron dimensions[1,2]. Instead of continuing to put more effort into the fabrication of smaller junctions and thus reducing the junction capacitance, it is also possible to implement integrated tuning elements, which are fairly easy to fabricate and result in a high sensitivity and broad bandwith. It has been shown that junctions with integrated tuning used in submm-wave mixers give good results[3,4].

The first published stub measurements used the self-pumped steps in the I-V characteristic to measure the resonance of the stub[5]. A more accurate and complete evaluation can be performed with a wide-band Michelson interferometer as first shown by Hu et. al.[6].

In this paper we first describe our design criteria for niobium stubs in combination with niobium junctions. Next, we describe how they can be analyzed on a log-periodic antenna with two 1 μm^2 junctions in series. Each junction has its own stub. Stubs for 100 GHz

and 350 GHz have been designed. The first type is expected to have multiple resonances from which the dispersion in niobium can be calculated. These antennas are made on 200 μm thick quartz substrates and on 7 μm silicon membranes. The results are used to separate stub and antenna resonances and to estimate the dispersion.

The organization of this paper is as follows: the theoretical background will be introduced in Sec.II, the fabrication results are presented in Sec.III, the experimental details are described in Sec.IV, the comparison between theory and experiment is discussed in Sec.V, and the conclusion will be drawn in Sec.VI.

II Model calculation.

To tune out the geometric capacitance an inductive tuning element was used. An example of the devices studied is shown in Fig.1. Two junctions in series, placed in the center of a log-periodic antenna, were used. To each junction a stripline type inductor is attached. The total arrangement can be modelled with the circuit shown in Fig.2. For completeness the connecting strip between the two junctions is included as an inductor L_{leads}. In practice this inductance is negligible in evaluating the frequency response.

Using integrated tuning, the junction impedance can not simply be described as a pure resistor with a parallel capacitor. Instead, it must be described as a capacitor in parallel with a complex admittance with a conductive part (G_Q) and a susceptive part (B_Q). Since the experiment works in the small signal limit and the Josephson effect is suppressed by a magnetic field, the junction admittance can be described as follows[7,8]:

$$G_Q = \frac{e}{2\,\hbar\cdot\omega}\cdot[\,I_{dc}(V_0 + \frac{\hbar\cdot\omega}{e}) - I_{dc}(V_0 - \frac{\hbar\cdot\omega}{e})\,] \qquad (1)$$

$$B_Q = \frac{e}{2\,\hbar\cdot\omega}\cdot[\,I_{kk}(V_0 + \frac{\hbar\cdot\omega}{e}) - 2\cdot I_{kk}(V_0) + I_{kk}(V_0 - \frac{\hbar\cdot\omega}{e})\,] \qquad (2)$$

These equations show that the resonant frequency depends on the bias voltage and the photon-energy. In these equations is $\hbar\omega/e$ the energy of the photon step, V_0 is the bias voltage, and

$$I_{kk} = P\int_{-\infty}^{\infty} \frac{dV'}{\Pi}\cdot\frac{I_{dc}(V') - \frac{V'}{R_n}}{V' - V} \qquad (3)$$

where I_{kk} is the Kramers-Kronig transform, which can be calculated from the dc-IV curve.

The inductance per unit length of the stub can be calculated as follows[9]:

$$L_s = \frac{\mu_0}{k\cdot w}\cdot[\,t_d + \frac{\lambda}{\tanh(\frac{t_1}{\lambda})} + \frac{\lambda}{\tanh(\frac{t_2}{\lambda})}\,] \qquad (4)$$

where w is the width of the stub, k is the fringing factor[10], t_1, t_2 and t_d are the thicknesses of the ground plane, the stub, and the dielectric layer respectivily, and λ is the penetration depth of the niobium layers. The capacitance per unit length of the stub is given by:

$$C_s = k\cdot\varepsilon_{eff}\cdot\varepsilon_0\cdot\frac{w}{t_d} \qquad (5)$$

Knowing the capacitance and the inductance of the stub, the impedance Z_0 and the phase velocity v_0 follow from the definitions:

$$Z_0 = \sqrt{\frac{L_s}{C_s}} \qquad (6)$$

$$v_0 = \frac{1}{\sqrt{L_s \cdot C_s}} \qquad (7)$$

The impedance of a transmission line with small loss and dispersion follows from:

$$Z = \frac{Z_0 \cdot \alpha \cdot l}{\sin^2(\frac{\omega \cdot l}{v_0})} + \frac{Z_0}{j \cdot \tan(\frac{\omega \cdot l}{v_0})} \qquad (8)$$

Where α is the loss per unit length and l is the length of the stub. The RF coupling

coefficient C_{RF} defined as the fraction of the available power dissipated in the junction

is given by:

$$C_{RF} = 1 - \left| \frac{Y_A - Y_J^*}{Y_A + Y_J} \right|^2 \qquad (9)$$

where $Y_A = 1/R_A$ is the simplified admittance of the antenna (1/120 Ω), and Y_J is the

admittance of the right hand side of Fig.2.

If both areas and stub lengths are equal then the resonant frequency can be

approximated from:

$$\omega \cdot C_j + \frac{1}{\omega \cdot X_s} + \frac{1}{\omega \cdot X_q} = 0$$

$$(10)$$

In our equations we do not take into account the behaviour of the log-periodic antenna,

this is rather complex and not known in all detail. Therefore it will be very difficult to

identify the loss from the observed resonances, because it could be loss in niobium, bad

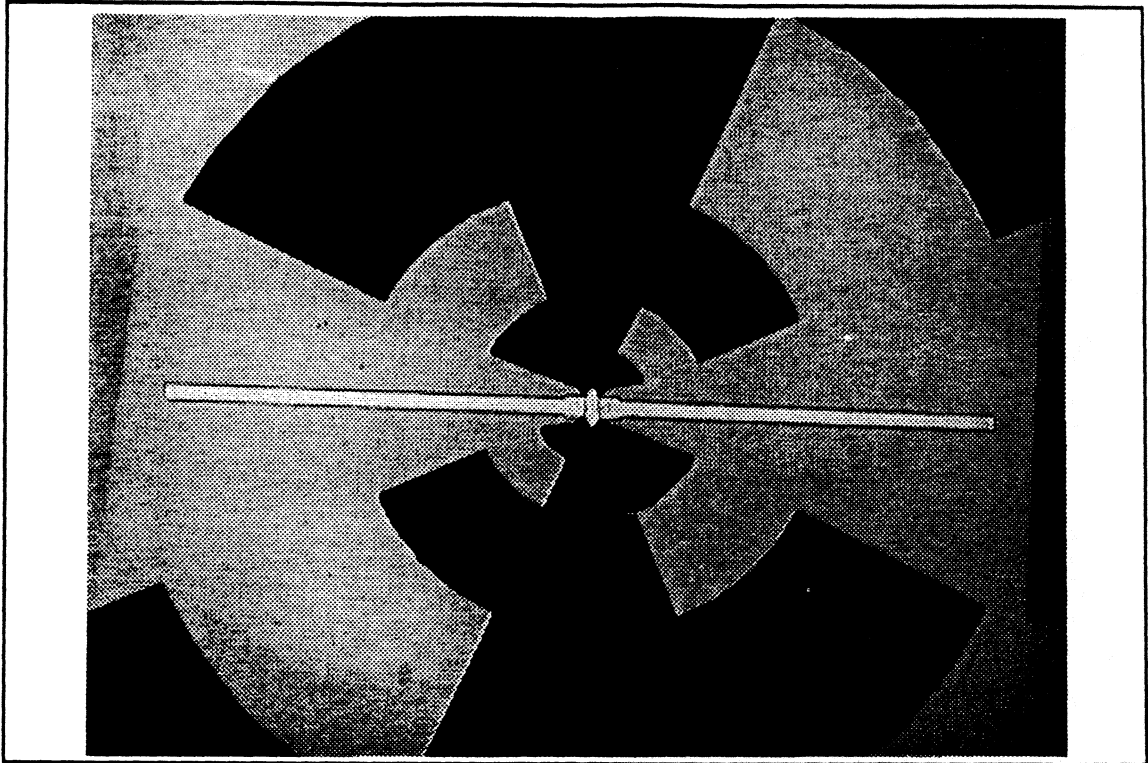coupling to the antenna or a combination of both.

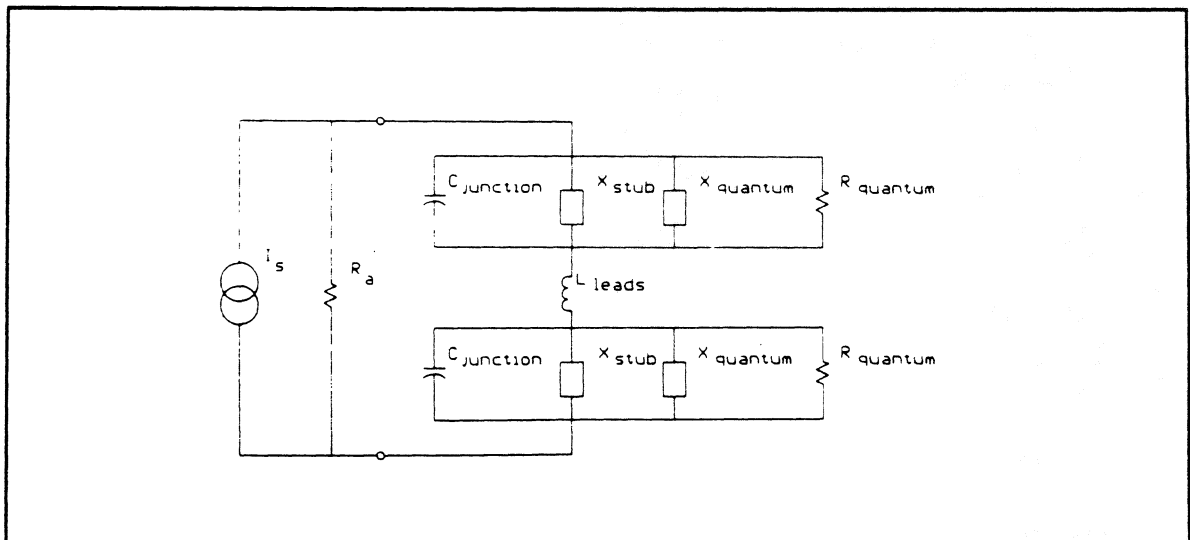Fig.1. Photo of a log-periodic antenna with two junctions in series. Each junction has its own stub.

Fig.2 Electrical equivalent of two junctions in series with integrated tuning elements.

III Fabrication of devices.

The detector is positioned in the center of a broad-banded log-periodic antenna. We used 2 junctions in series of each 1 μm^2 and a current density of 12000 A/cm². On top of the junctions the wiring layer was defined with a stub for each junction (Fig.1.). The dielectric layer between the ground plane (antenna) and the stub was 250 nm thick sputtered SiO_2. The junctions have been fabricated with the Selective Niobium Over-Etch Process (SNOEP)[11].

Antennas have been fabricated on 200 μm thick quartz substrates and on 7 μm thick silicon membranes (Fig.3.). The membranes have been etched in ethylenediamine-pyrocatechol-water (EPW)[12]. The junctions on the membranes were fabricated after the etching of the membranes. With the obtained thickness, the membrane is transparent which simplifies the alignment of the antenna on the membrane.

Two different stub lengths were fabricated for different purposes. Firstly, short stubs (around 120 μm) were designed to resonate at 350 GHz. A single resonance simplifies the comparison with the model and it can easily be implemented in the waveguide mixer chip design. Secondly, long stubs (around 500 μm) were designed to have a fundamental resonance around 100 GHz and multiple resonances at higher frequencies. From the frequencies of the resonances in principle the dispersion and loss in niobium can be estimated.
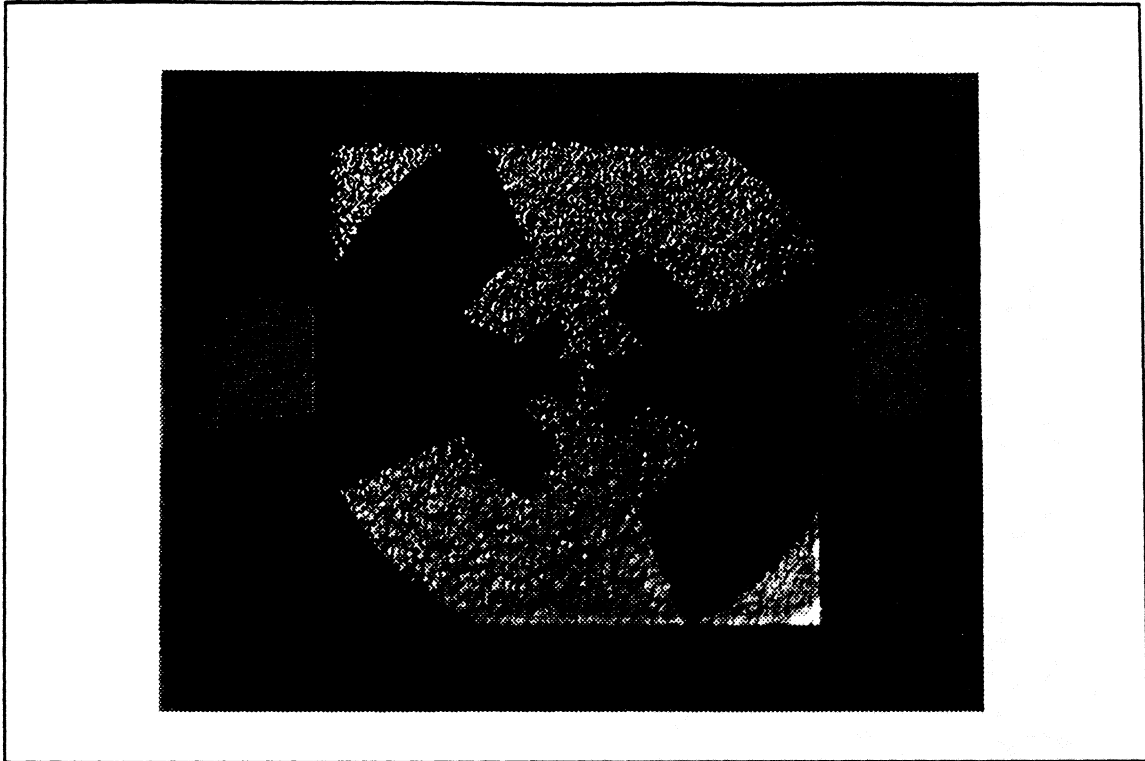
Fig.3. Photo of the antenna fabricated on a 7 μm thick silicon membrane.

IV Measurement set-up

For measuring the response of the detector, we used a Michelson interferometer with a Hg arc lamp as source[13] (Fig.4.). The operating frequency range was determined by a 50 μm thick kapton film beam-splitter. The mechanical traveling distance was 50 mm resulting in a resolution of 4 GHz. Both single sided and double sided interferograms were measured. An example of the resulting spectra with multiple resonances is plotted in Fig.5.

The antenna was mounted in a liquid helium dewar with dc-bias connections. Since the
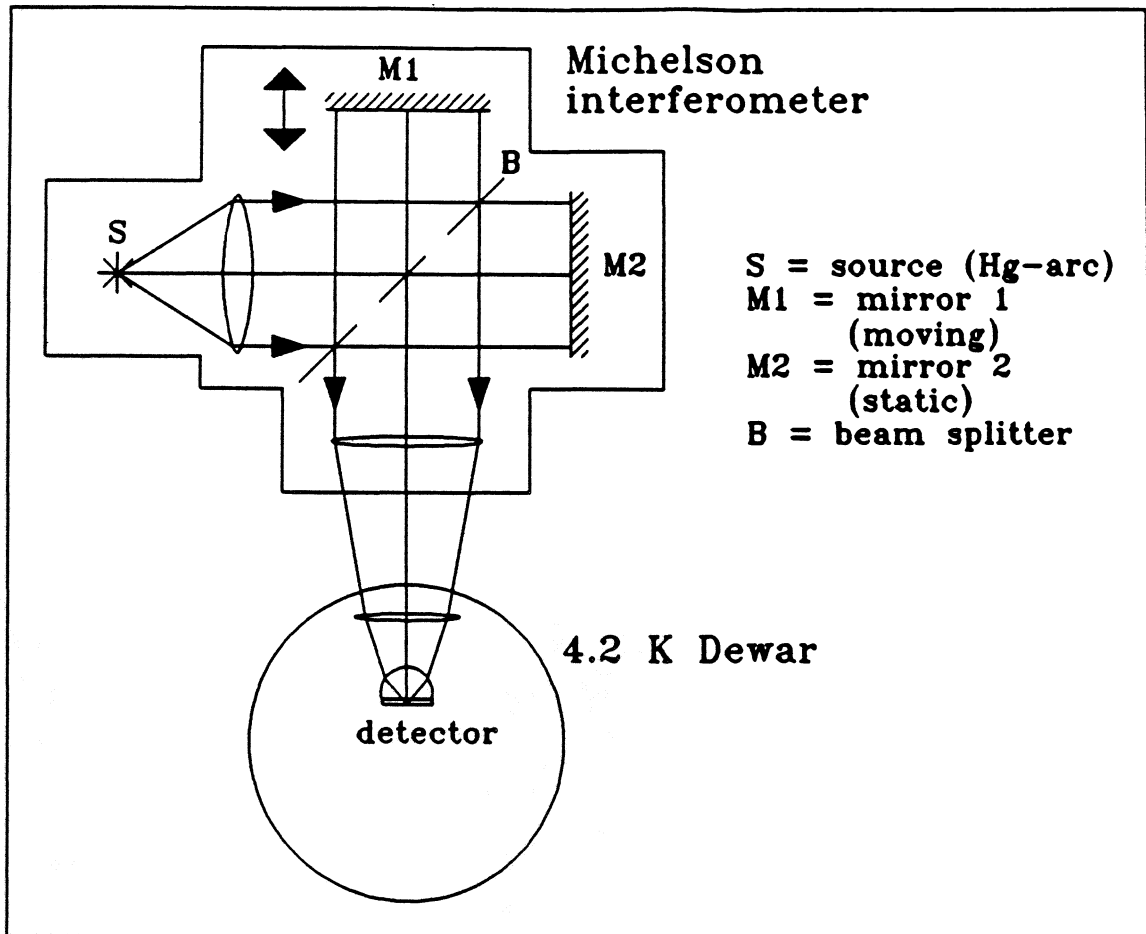
Fig.4. Schematic of the Michelson interferometer.

Michelson was not under vacuum during the measurement, the water absorption lines at 380 GHz, 448 GHz, 557 GHz and 752 GHz were visible when sufficient resolution was used. All antennas fabricated on a quartz substrate were glued to a quartz hyper-hemispherical lens. The lens optimizes the optical coupling and results in a better sensitivity. We have also performed measurements with the log-periodic antenna on a thin membrane. In that case no lens was used, resulting in a much lower signal. By using longer integration times we could improve the signal to noise ratio to an acceptable level.
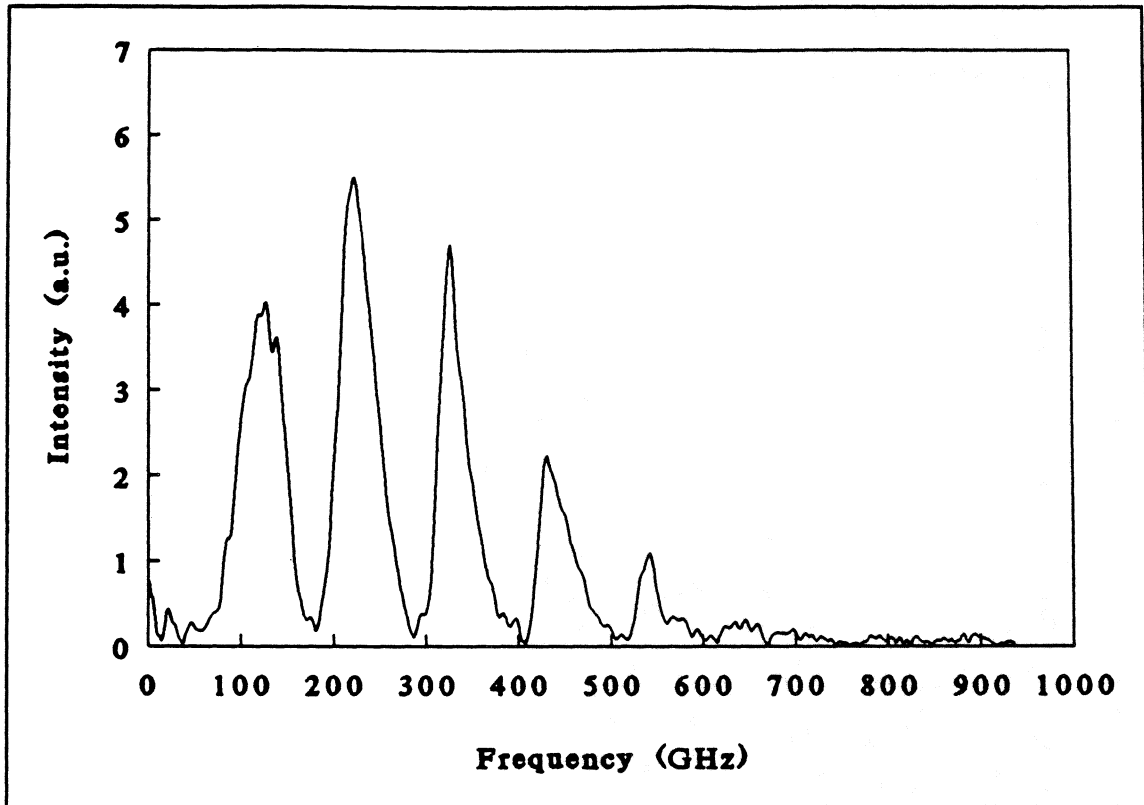
Fig.5 Spectrogram of a device with multiple resonances.

V Results

A: Short stubs on 200 μm quartz substrates.

Antennas with stub lenghts around 120 μm were investigated to determine the specific capacitance of the junction and the penetration depth of the niobium layers. Resonant frequencies were measured from two different batches. The resonant frequency is depending on the bias voltage due to the behaviour of the quantum impedance (eq.1 and eq.2). Calculated and measured results are shown in Fig.6. Best agreement between

theory and experiment was obtained with the assumption of a specific capacitance of 55 fF/μm^2 and a penetration depth of 100 nm. These values were further used in calculations of the long stubs. Differences between calculations and measurements are due to the noise in the spectrogram which complicates the determination of the resonant frequencies. No multiple resonance is observed.
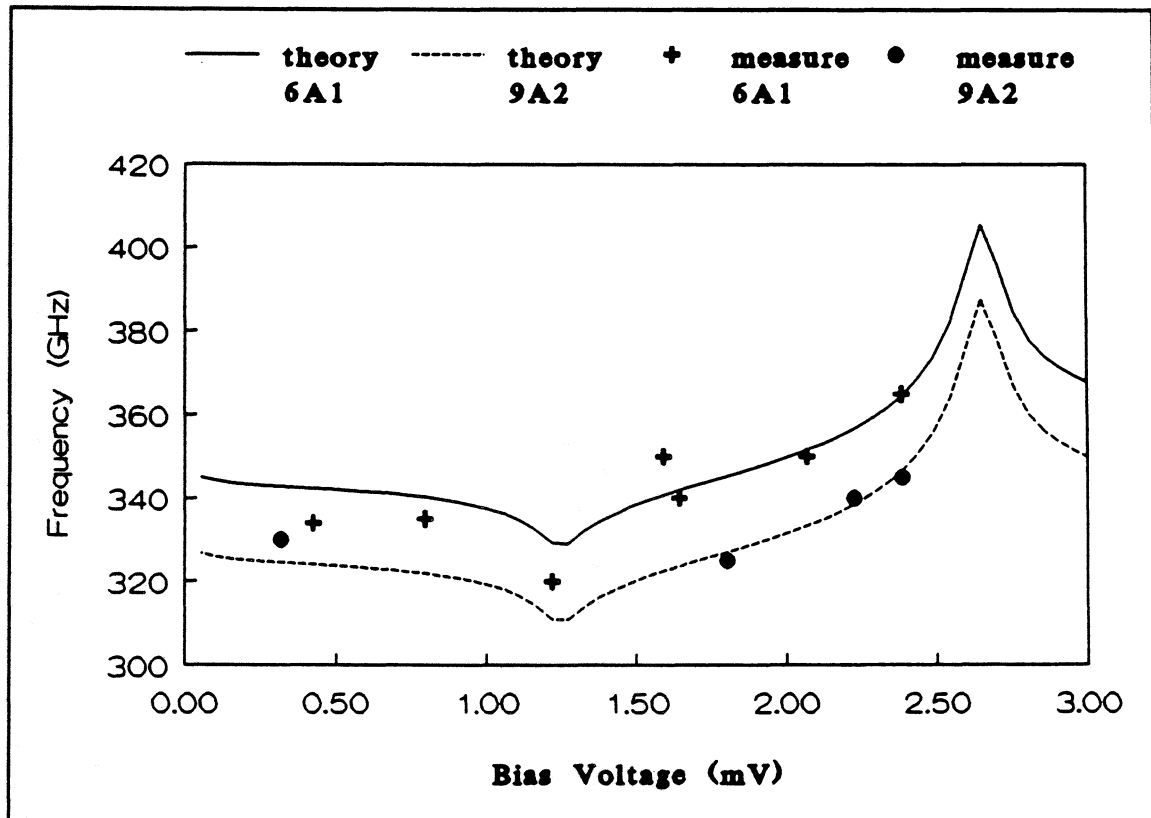

Fig.6 Calculated and measured resonant frequencies as a function of bias voltage for two different junction batches.

B: Long stubs on 200 μm quarz substrates.

Next, the resonances of a 527 μm long stub on a quartz substrate were measured. The results of the measurements at different bias voltages are plotted in Fig.7 and are

compared with model calculations. At the first two resonances the measurements agree fairly well with the model both below as well as above the gap voltage. The two higher resonances have a larger frequency shift close to the gap than the model predicts. More measurements with different lengths are planned for a more detailed evaluation. Stub resonances up to 580 GHz are observed, while no antenna resonances are visible. We do not see any dispersion in the resonances of the stubs (Fig.5).
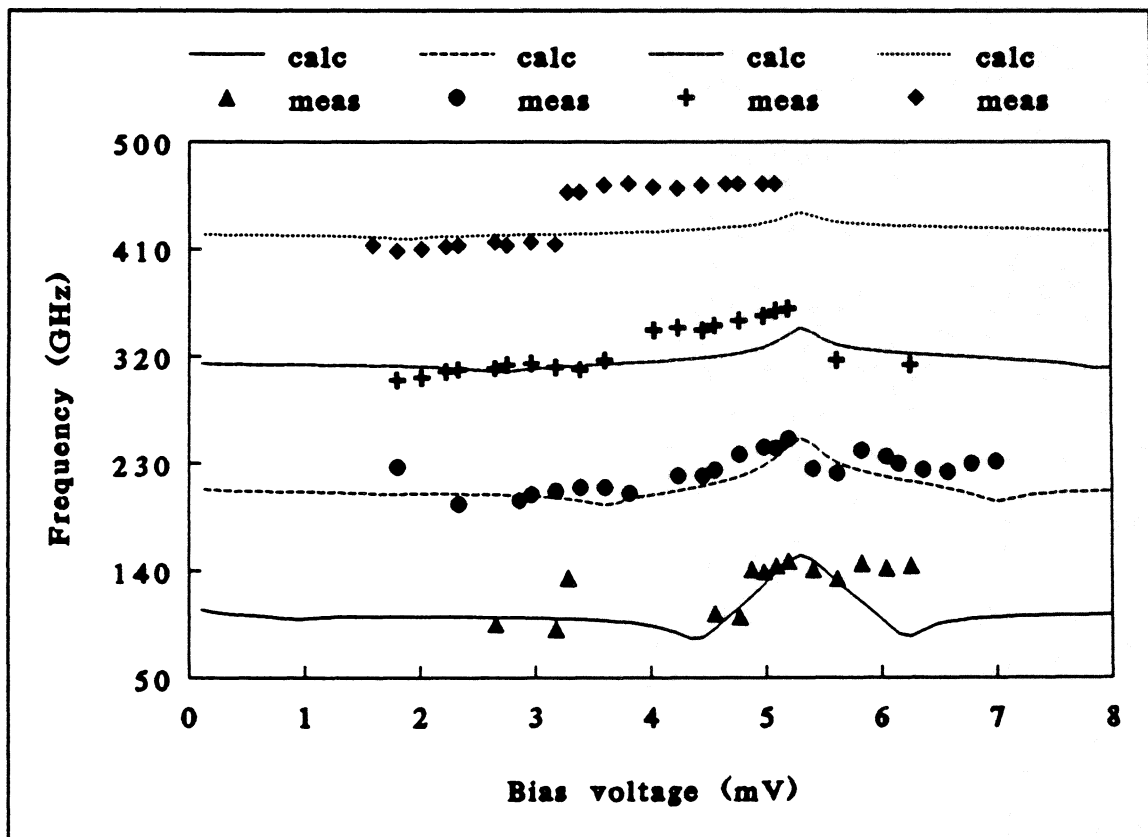

Fig.7 Calculated and measured resonant frequencies for an antenna with a 527 μm long stub on a quartz substrate as a function of bias voltage.

C: Long stubs on 7 μm silicon membranes.

The resonances of a 527 μm long stub on a 7 μm thick silicon membrane were measured. A double sided interferogram was used to decrease the noise in the spectrogram. The resolution (8 GHz) is lower because of the decreased scan length. The effect of the quantum susceptance is not clearly observed because of the loss in resolution and signal. We measured stub resonances at 110, 200 and 325 GHz. Incidentally resonances at 165, 310 and 540 GHz occur which are probably substrate resonances. The highest stub resonance appears to be at 450 GHz which is lower than the measurements on quartz. The lowest three resonances are compared with the model calculations in Fig.8. It is not clear why above 330 GHz no well defined resonances occur except for the substrate resonance at 540 GHz.
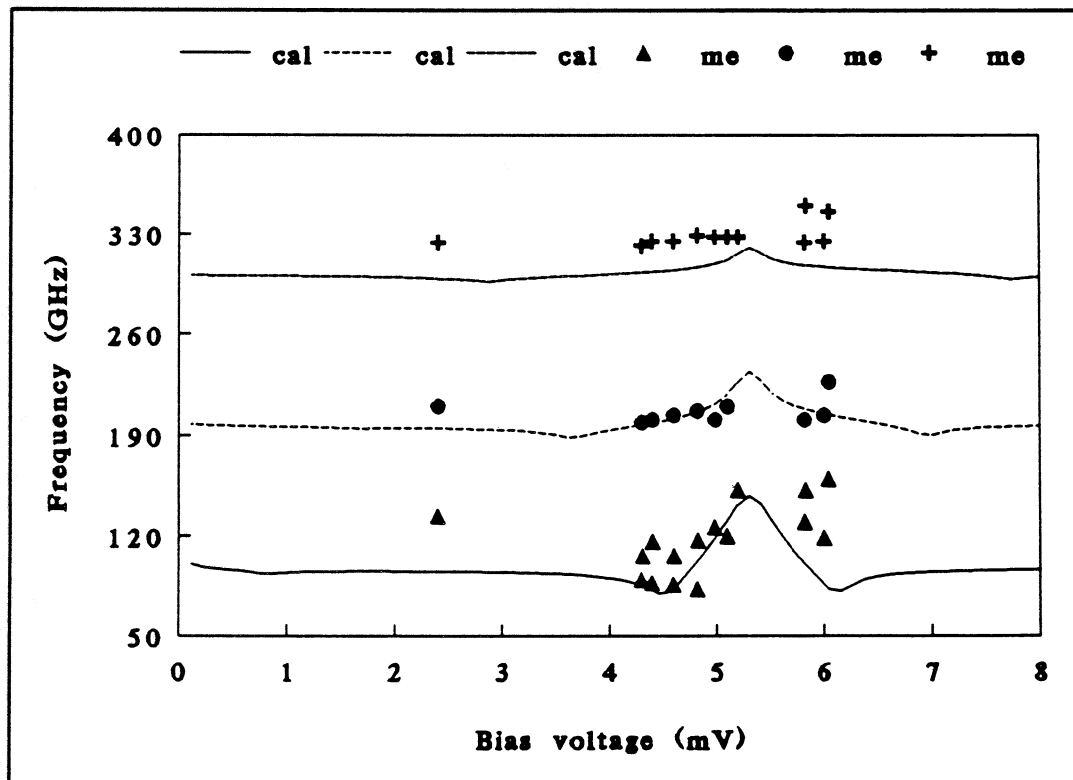

Fig.8 Calculated and measured resonance frequencies for a 527 μm long stub on a silicon membrane as a function of bias voltage.

VI Conclusions

The theoretical model and the experimental results for the short stubs lead to a penetration depth of 100 nm and a specific capacitance of 55 fF/μm^2. This is independent of the measured batch. For long stubs the model predicts a different behaviour at higher resonances than is measured. The measured frequency shift at the higher resonances is larger than the model predicts. Both below and above the gap voltage the resonances agree fairly well with the model. Resonances up to 580 GHz are observed. For antennas fabricated on 7 μm thick silicon membranes resonances up to 480 GHz are observed. Also possible substrate resonances are measured. No resonances above 600 GHz are observed, which is close to the gap frequency of niobium (650 GHz).

Acknowledgements

References

1. W.R. McGrath, H.H.S. Javadi, S.R. Cypher, B. Bumble, B.D. Hunt, and H.G. LeDuc, Proceedings of *Second International Symposium on Space TeraHertz Technology*, 423 (1991)

2. J.W. Kooi, M. Chan, T.G. Phillips, B. Bumble, and H.G. LeDuc, Proceedings of *Second International Symposium on Space TeraHertz Technology*, 459 (1991)

3. A.W. Lichtenberger, D.M. Lea, A.C. Hicks, J.D. Prince, R. Densing, D. Peterson, and B.S. Deaver, Proceedings of *Second International Symposium on Space TeraHertz Technology*, 439 (1991)

4: J. Zmuidzinas, and H.G. LeDuc, Proceedings of *Second International Symposium on Space TeraHertz Technology*, 481 (1991)

5. A.V. Räisänen, W.R. McGrath, P.L. Richards, and F.L. Lloyd, IEEE Trans Microwave Theory Tech. 33, 1495 (1985)

6. Q. Hu, C.A. Mears, P.L. Richards, and F.L. Lloyd, Int. J. of Infrared and MM Waves, 9, 303 (1988)

7. J.R. Tucker, and M.J. Feldman, Rev. Mod. Phys. 57, 1055 (1985)

8. Q. Hu, C.A. Mears, P.L. Richards, and F.L. Lloyd, Phys. Rev. B, 42,10250 (1990)

9. J.C. Swihart, J. Appl. Phys. 32, 461 (1961)

10. W.H. Chang, J. Appl. Phys. **50**, 8129 (1979)

11. M.M.T.M. Dierichs, R.A. Panhuyzen, C.E. Honingh, M.J. de Boer, and T.M. Klapwijk (unpublished results)

12. K.E. Petersen, Proc. of the IEEE **70**, 420 (1982)

13. P.L. Richards, in *Spectroscopic Technique for Far Infrared Submillimeter and Milimeter Waves*, (North-Holland, Amsterdam, 1967)